Physically-based model for gully simulation: Application to the Brazilian Semiarid Region

Pedro Henrique Lima Alencar[1,2], José Carlos de Araújo[2], and Adunias dos Santos Teixeira[2]

[1]TU Berlin, Institut für Ökologie, 10587 Berlin, Germany

[2]Federal University of Ceará, Departamento de Engenharia Agrícola, Fortaleza, Brazil

Correspondence: Pedro Alencar (pedro.alencar@campus.tu-berlin.de); José Carlos de Araújo (jcaraujo@ufc.br)

Abstract. Gullies lead to land degradation and desertification as well as increasing environmental and societal threats, especially in arid and semiarid regions. Despite this fact, there is a lack of research initiatives. As an effort to better understand soil loss in these systems, we studied small permanent gullies, a recurrent problem in the Brazilian Northeastern semiarid region. The increase of sediment connectivity and reduction of soil moisture, among other deleterious consequences, endanger this desertification-prone region and reduce its capacity to support life and economic activities. Thus, we propose a model to simulate gully-erosion dynamics, derived from the previous physically-based models by Foster and Lane and by Sidorchuk. The models were adapted so as to simulate long-term erosion. A threshold area shows the scale dependency of gully erosion internal processes (bed scouring and wall erosion). To validate the model, we used three gullies ageing over six decades in an agricultural basin in the State of Ceará. The geometry of the channels was assessed using Unmanned Aerial Vehicle and Structure-from-Motion technique. Laboratory analyses to obtain soil properties were performed. Local and regional rainfall data were gauged to obtain sub-daily rainfall intensities. The threshold value (cross-section area of 2 m^2) characterises when erosion in the walls, due to loss of stability, becomes more significant than sediment detachment in the wet perimeter. The 30-minute intensity can be used when no complete hydrographs from the rainfalls are available. Our model could satisfactorily simulate the gully-channel cross-section area growth over time, yielding Nash-Sutcliffe efficiency of 0.85 and R^2 of 0.94.

1 Introduction

On our way to sustainable development and environmental conservation, soil erosion by water was pointed out as a key problem to be faced in the 21st century (Borrelli et al., 2017; Poesen, 2018). The impact of water-driven soil erosion, on the economy and food supply alone, represents an annual loss of US$ 8 to 40 billion, a cut in food production of 33.7 million tonnes and an increase in water usage by 48 km^3. These effects are felt more severely in countries like Brazil, China and India as well as low-income households worldwide (Nkonya et al., 2016; Sartori et al., 2019). Estimates on total investments to mitigate land-degradation effects on site (e.g. productivity losses) and their off-site effects (e.g. biodiversity losses, water body siltation) lead

to more alarming values, averaging US$ 400 billion yr^{-1} (Nkonya et al., 2016). Nonetheless, these values were obtained by studies of soil loss using USLE (Universal Soil Loss Equation) or similar methods, with none considering gully erosion. Thus, the real economical and social impacts of soil erosion are not completely comprehended as long as we do not better understand gully erosion and how to model it.

Notwithstanding, soil degradation had already been an issue since the early 20^{th}-century, having been, for instance, reported by the USDA and the National Conservation Congress, with over 44 thousand km^2 of abandoned land due to intense erosion. By the end of the 1930s, this number had increased to over two hundred thousand km^2 (Montgomery, 2007). Among soil erosion mechanisms, gully erosion plays a relevant role in sedimentological processes in watersheds since it frequently is the major source of sediment displacement (Vanmaercke et al., 2016). Ireland et al. (1939) observed the effect of intense land-use change on gully formation early, mainly due to changes of land-cover and flow path direction. These landscape modifications were connected to runoff acceleration and/or concentration, therefore, triggering gullies.

Gully erosion consists of a process that erodes one (or a system of) channel(s) that starts mainly due to the concentration of surface water discharge erosion during intense rainfall events (Bernard et al., 2010). The concentrated flow causes a deep topsoil incision and may reach the groundwater table and sustain the process (Starkel, 2011). Gullies are a threshold-controlled process (Conoscenti and Rotigliano, 2020) and their initiation is connected to anthropogenic landscape modifications as well as land use and land cover changes, as observed in the other tropical biomes (Katz et al., 2014; Hunke et al., 2015; Poesen, 2018). On the other hand, the presence of vegetation may prevent soil erodibility both by increasing cohesion forces and enhancing soil structure (Vannoppen et al., 2017). Maetens et al. (2012) suggested that land-use changes lead to runoff changes and, hence, directly affect erosive processes. Gully erosion can also be affected by climate change, e.g., an increase in rainfall intensity could lead to higher erosive potential (Figueiredo et al., 2016; Panagos et al., 2017). Gullies are strongly dependent on landscape factors. With the advance of machine-learning techniques and the use of large data sets, some of the factors that mostly influence gully formation were identified, such as lithology, land use and slope. Some indexes were also pointed out as relevant to indicate gully initiation, such as the Normalized Difference Vegetation Index, Topography Wetness Index and Stream Power Index (Arabameri et al., 2019; Azareh et al., 2019; Conoscenti and Rotigliano, 2020).

Gullies play a relevant role in the connectivity of catchments (Verstraeten et al., 2006), allowing more sediment to reach water bodies and, thus, increase siltation (de Araújo et al., 2006). For being particularly relevant among the erosion processes, gullies execute a great pressure on landscape development: they change the water-table height, alter sediment dynamics and increase runoff (Valentin et al., 2005; Poesen, 2018; Yibeltal et al., 2019). They represent an increasing risk to society and environment for affecting land productivity, water supply, floods, debris flow and landslides (Liu et al., 2016; Wei et al., 2018). Gullies also have a large impact on the economy due to high mitigation costs, a reduction of arable fields, a decrease of groundwater storage, an increase of water and sediment connectivity and more intense reservoir siltation (Verstraeten et al., 2006; Pinheiro et al., 2016). The assessment of gully impacts on production costs in an arid region of Israel showed that costs of gully mitigation represent over 5% of total investments, and production losses are as large as 37 % (Valentin et al., 2005).

The State of Ceará, located in the semiarid region, has its total area (over 148,000 km^2) included in the risk zone of desertification. From this total, about 11.5% is also under advanced land degradation conditions, including the formation of Badlands

and Gullies, a similar condition to the one found in other desertification hotspots in the semiarid (Mutti et al., 2020). The region is also especially vulnerable to climate change (Gaiser et al., 2003), and both degradation and desertification can be accelerated by gullies (Zweig et al., 2018). The Brazilian semiarid region is also characterised by shallow crystalline rock bed with scarce groundwater and baseflow, which makes its population rely almost exclusively upon superficial reservoirs for water supply (Coelho et al., 2017). Therefore, gullies are a two-way threat, first, by depleting the already scarce groundwater and second, by increasing sediment connectivity, causing siltation and resulting in loss of storage capacity and water quality (Verstraeten et al., 2006).

Despite their relevance to hydro-sedimentological processes, gullies are often neglected in models (Poesen, 2018), and should be directly addressed (Paton et al., 2019). However, gully erosion is a process with the interaction of many variables, with several of them difficult to assess (Bernard et al., 2010; Castillo and Gómez, 2016). According to Bennett and Wells (2019), for instance, no model has ever been presented to clearly explain the process of gully formation. Among the models that do consider gully erosion, the use of empirical approach prevails (e.g. Thompson, 1964; Woodward, 1999; Nachtergaele et al., 2002; Wells et al., 2013); whereas others focus primarily on physically-based algorithms (e.g. Foster and Lane, 1983; Hairsine and Rose, 1992; Sidorchuk, 1999; Dabney et al., 2015).

It is, therefore, an important milestone to understand how gully erosion starts and develops (Poesen, 2018). The objective of this work is to propose a physically-based model that predicts growing dynamics and sediment production in small permanent gullies on a hillslope scale. In order to achieve this, we tested two models – Foster and Lane (1983) and Sidorchuk (1999) – and two adapted models, one being the modification of the model of Foster and Lane and the other the coupling of both models. To validate the model, we selected three small permanent gullies in the State of Ceará. The gullies' geometry was assessed using UAV (Unmanned Aerial Vehicle) and the soils were sampled and characterised.

We understand small permanent gullies to be the result of active erosive processes that form channels by concentrated flow and do not interact with groundwater. Normally, these gullies could be remedied by regular tillage processes, but in abandoned or unclaimed land,they usually remain untreated for long periods. Although the land where they develop is usually unused for economic activities besides livestock grazing in open range, the development of such gullies threatens the ecosystem and community.

2 MATERIALS AND METHODS

2.1 Study area

The Brazilian Semiarid Region (1 million km^2) is mainly covered by the Caatinga biome with vegetation characterised by bushes and broadleaf deciduous trees (Pinheiro et al., 2013). The region is prone to droughts and highly vulnerable to water scarcity (Coelho et al., 2017). More than 25 million people live in this region where agriculture (maize, beans, cotton) and livestock in the open range are of utmost socio-economic relevance. Usually, rural communities use deleterious practices, such as harrowing and field burning, which enhance the risk of intense erosive processes. These characteristics lead to a scenario of soil erosion and water scarcity with high social, economic and environmental consequences (Sena et al., 2014). Erosion in

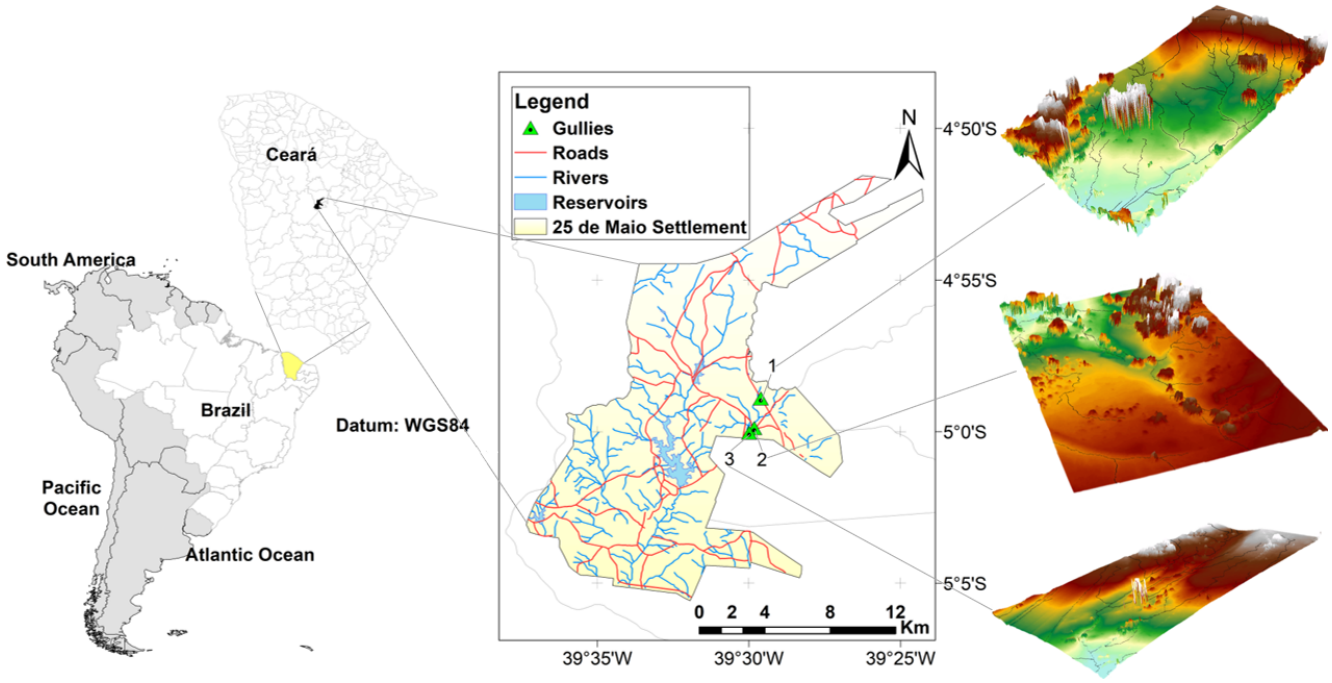

Figure 1. Location of the study area and the gully sites (gullies 1, 2 and 3) and the digital elevation models. The roads, rivers and reservoirs were mapped by Silva et al. (2015).

general (and gullies in particular) increases local water supply vulnerability due to reservoir siltation (de Araújo et al., 2006) and water-quality depletion (Coelho et al., 2017).

The study area is located in the Madalena Representative Basin (MRB, 75 km^2, State of Ceará, Northeastern Brazil; see Figure 1), located in the Caatinga biome, a dry environment with a semiarid hot BSh climate, according to the Köppen classification. The annual precipitation averages 600 mm, concentrated between January and June (Figure 2), and the potential evapotranspiration totals 2,500 mm yr^{-1}. Geologically, the basin is located on top of the crystalline bedrock with shallow soils and limited water storage capacity. The rivers are intermittent and runoff is low, typically ranging from 40 to 60 mm yr^{-1} (Gaiser et al., 2003). The basin is located within a land reform settlement with 20 inhabitants per km^2, whose main economic activities are agriculture (especially maize), livestock and fishing (Coelho et al., 2017; Zhang et al., 2018).

Three gullies were selected for this study, all located on the eastern portion of the basin. The studied gullies have the following dimensions (average $\pm$ standard deviation): projection area (317 $\pm$ 165 m^2), length (38 $\pm$ 6 m), volume (42 $\pm$ 25 m^3), depth (0.44 $\pm$ 0.25 m) and eroded mass (61 $\pm$ 36 Mg). The coordinates are presented in Table 1. Despite their small sizes, they possess a significant impact on the landscape for reducing productive areas and soil fertility. According to the information obtained from local villagers, gully erosion started immediately after the construction of a country road in 1958 (Figure 3). Before the construction, the sites were covered by Caatinga vegetation (Pinheiro et al., 2013). The road modified the natural

drainage system and does not provide for any side nor outlet ditches, therefore generating a concentrated runoff at its side. This has caused excessive runoff on the hillslopes and triggered gully erosion.

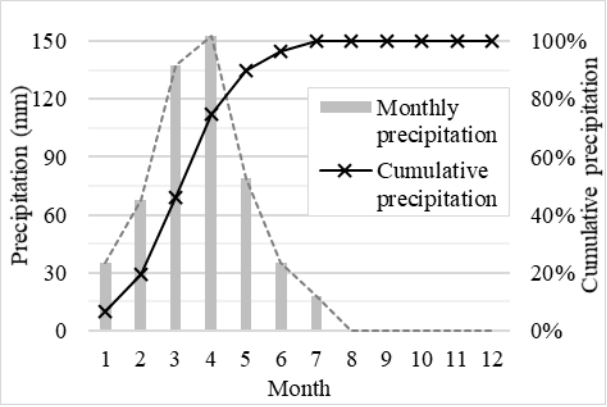

Figure 2. Monthly precipitation (median) and cumulative precipitation at MRB from 1958 to 2015.

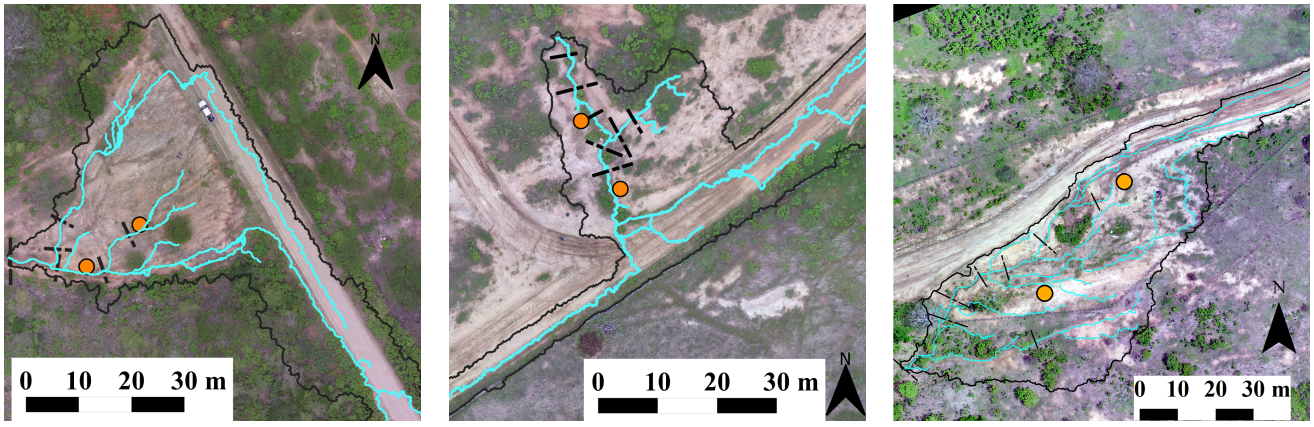

(a) (b) (c)

Figure 3. Aerial photogrammetry of the studied gullies. Note that they are at the margin of the road, receiving the concentrated flow diverged from it. The continuous black line represents the catchment boundaries; the blue line represents the flow paths; the dashed black lines are the cross-sections used on the validation of the model; and the orange dots are the soil sampling points - (a) gully 1; (b) gully 2; (c) gully 3.

Table 1. Coordinates of the three gullies used in this study (Datum: WGS84).

Area	Latitude	Longitude
Gully 1	04°58’54.3"S	39°29’36.4"W
Gully 2	04°59’53.1"S	39°29’49.4"W
Gully 3	05°00’02.4"S	39°29’59.4"W

2.2 Topography survey

The assessment of the gully data was achieved using an Unmanned Aerial Vehicle (UAV), a technique applied in other regions as well (Stöcker et al., 2015; Wang et al., 2016; Agüera-Vega et al., 2017). A UAV equipped with a 16 MP camera (4000 x 4000 pixels) and field of view of 94 % was used. The flight was at 50 m altitude with a frontal overlap of 80 % and lateral overlap of 60 %. For the geo-reference of the mosaic, five ground control points were deployed which were evenly distributed in each area, both in the high and low ground. The coordinates were collected using a stationary GNSS – RTK (L1/L2) system with centimetre-level accuracy.

The Digital Surface Model was produced using the Structure from Motion technique. This process consists of a three-dimensional reconstruction of the surface, derived from images and the generation of a dense cloud of 3D points based on the matching pixels of different pictures and Ground Control Points (GPCs); the processing result is a model as accurate as one obtained by laser surveys (e.g., Light detection and ranging - LiDAR), but cheaper and less time consuming (Stöcker et al., 2015; Agüera-Vega et al., 2017). The ground sample distance (pixel size) obtained is four to five centimetres and the digital models have high precision, with a vertical position error of one centimetre and horizontal error of six millimetres. The vegetation, yet sparse, was an obstacle to increasing the quality of the survey. However, as the focus of this study was the gully cross-section geometry, vegetation interference was acceptably low.

2.3 Soil data

Due to the scale of this experiment and the homogeneity of the soil-vegetation components (Güntner and Bronstert, 2004), we divided the areas into two sets based on grain-size distribution, organic matter and bulk density. Gully 1 (G1) has specific features and comprises the first soil (S1), whereas gullies G2 and G3, close to each other, are represented by the second soil (S2).

At the gully sites, soil surveys were carried out to assess the properties and parameters required to implement the model; undisturbed soil samples were collected (see Figure 3) at depths of 0.10 m, 0.30 m and 0.50 m (two sites, three depths, three samples per depth, totalling 18 samples collected). At the depth of 0.50 m, a well-defined horizon C, rich in rocks and soil under formation, was identified. The maximum depth of the non-erodible layer ranged from 60 to 75 cm in all gullies. We performed grain-size distribution, sedimentation, organic matter, bulk density and particle density analysis.

The soils are loamy, with clay content ranging from 6 % to 37 %. The particle density is 2580 kg m^{-3}. The soils are Luvisols and have a typical profile, with the top layer relatively poor in clay when compared to the layers below and with the regular occurrence of gravel at the surface. Furthermore, Luvisols are rich in active clay, which makes them prone to form cracks and macropores when dry (dos Santos et al., 2016), a process also documented in soils with similar texture in a semiarid area in Spain (van Schaik et al., 2014). Rill erodibility values (K_r) and critical shear stress (τ_c) for the soils were obtained using the Equations 1 and 2 (Alberts et al., 1995) and are also presented in Table 2.

$$K_r = 0.00197 + 0.00030\%VFS + 0.038633e^{(-1.84\%OM)} \quad (1)$$

Table 2. Grain-size distribution, organic matter for both soils (S1 - for the gully 1 - and S2 - for the gullies 2 and 3) at three depths (10, 30 and 50 centimetres) and the respective texture classification (USDA); and the estimated (in italic) rill erodibility (K_r) and critical shear stress (τ_c of the site soils) obtained using Equations 1 and 2.

Soil and layer	Gravel > 2 mm	FCS[a] > 0.1 mm	VFS[b] > 0.05 mm	Silt > 0.002 mm	Clay < 0.002 mm	Organic Matter	Bulk density (kg m^{-3})	Soil Class	K_r (s.m^{-1})	τ_c (Pa)
S1-10	13 %	45 %	21 %	11 %	10 %	3.1 %	1699	Sandy Loam	*0.015*	*2.102*
S1-30	6 %	46 %	16 %	14 %	18 %	3.3 %	1677	Sandy Loam	*0.016*	*2.912*
S1-50	4 %	63 %	20 %	7 %	6 %	2.2 %	1765	Loamy Sand	*0.020*	*1.900*
S2-10	17 %	33 %	22 %	11 %	17 %	4.9 %	1509	Sandy Loam	*0.012*	*2.499*
S2-30	8 %	29 %	6 %	20 %	37 %	5.7 %	1572	Clay Loam	*0.011*	*4.611*
S2-50	2 %	28 %	15 %	20 %	25 %	1.4 %	1643	Loam	*0.014*	*3.425*

[a] Fine to Coarse Sand; [b] Very Fine Sand.

$$\tau_c = 2.67 + 0.065\%C - 0.058\%VFS \quad (2)$$

where $\%VFS$ is the percentage of very fine sand, $\%C$ is the percentage of clay and $\%OM$ is the percentage of organic matter.

2.4 Rainfall data

Daily rainfall data for the location spanning the entire period was provided by the Foundation of Meteorology and Water Resources of Ceará (Funceme). We used five rain-gauge stations in the region, covering the period from 1958 to 2015. The annual rainfall in the area averages 613 mm (Supplementary material - Fig. S1) with a coefficient of variation of 43%, being typical values for the Brazilian Semiarid Region (de Araújo and Piedra, 2009). The double mass method was employed to check data consistency (Supplementary material - Fig. S2). The gaps in the measurements (January 1958 and September 1960) were filled by the nearest gauging station.

The modelling of the gullies is based on peak discharge, which demands sub-daily rainfall data, but only daily precipitation was available inside the study basin covering the whole experiment period. To proceed with the modelling, correlation curves relating total daily precipitation and rainfall intensity were used. In order to define which was the best intensity to be used in the modelling, four were tested (Figure 4) as input for the model: average (I_{av}), sixty-minute maximum (I_{60}), thirty-minute maximum (I_{30}) and fifteen-minute maximum (I_{15}) intensities.

To build such curves, we used data from the Aiuaba Experimental Basin's (AEB). This basin has been monitored since 2005 (Figueiredo et al., 2016) and has detailed hydrographs, with 5-minute temporal resolution. This experimental basin is located 190 km south of MRB and both basins are climatically homogeneous (Mendes, 2010). In addition, Figure 4 shows the rainfall data for the MRB collected during the rainy season in 2019 (January to July). We can observe that the data has similar

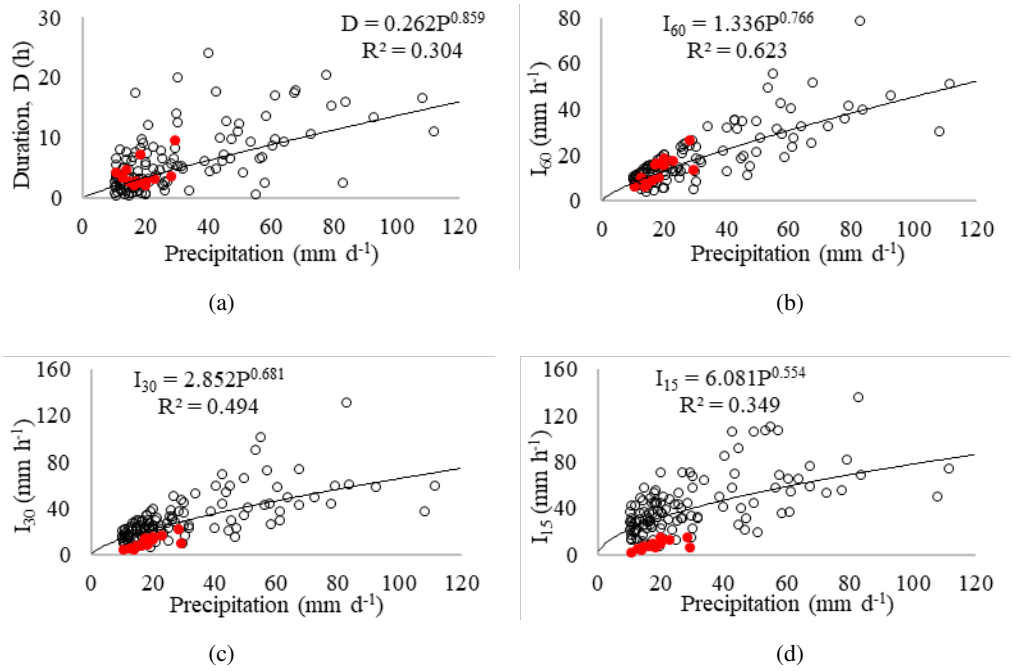

Figure 4. Correlation between daily precipitation and sub-daily variables at the Aiuaba Experimental Basin (Figueiredo et al., 2016). (a) daily precipitation versus event duration (D); (b) daily precipitation versus 60-minute maximum intensity (I_{60}); (c) daily precipitation versus 30-minute maximum intensity (I_{30}); and (d) daily precipitation versus 15-minute maximum intensity (I_{15}). The white circles indicate data obtained in Aiuaba from 2005 to 2014. The red dots indicate precipitations measured in the MRB from January to July 2019 (rainy season).

behaviour but is constantly on the lower area of the plot. It is relevant to note that in the year of 2019 in MRB it was dry (total annual precipitation of 402 mm, over 30 % lower than the average) and such behaviour was expected.

To obtain discharge values from intensity, we used the SCS-CN method (Chow, 1959). For the models, the main rainfall related variables are the event peak discharge and its respective duration. Because the gully catchment areas were small, their respective concentration time was negligible compared with the intense-rainfall duration in the region (Figueiredo et al., 2016), yielding a uniform pattern of peak discharge.

2.5 Gully modelling

To model small permanent gullies, we propose two models based in classical formulations from the literature of Foster and Lane (1983) and Sidorchuk (1999). The Foster and Lane Model (FLM) is one of the most used models of gully erosion based on net shear stress and transport capacity. The FLM assumes a rectangular cross-section and was originally designed for single rainfall ephemeral gully modelling. The Sidorchuk Model (SM) considers the mass balance of sediments, shear stress (in terms of critical velocity), soil cohesion and the Manning equation to estimate the cross-section geometry and channel slope. It also uses empirical equations based on field measurement to estimate the flow depth and width. This model gives special attention

to the processes involving gully wall transformation. A description of both models is available in the literature and in the supplement materials of this paper.

The proposed models are the Adapted Foster and Lane Model (FLM-λ) and the coupled model Foster and Lane & Sidorchuk Model (FL-SM). The key difference between the two proposed models is the amount of data required to use each one. The models are presented below.

2.5.1 Adapted Foster and Lane Model (FLM-λ)

The Foster and Lane Model (FLM), as proposed by its authors, considers a single source of erosion: the soil detached from the channels bed and walls due to shear stress. Field observation and literature (Blong and Veness, 1982), however, show that wall instability and failure can represent a significant source of sediment. To estimate the effect of wall erosion at the studied site, we proposed an empirical parameter (λ – Eq. 3) to correct the effect of lateral flow and wall erosion. This multiplicative parameter was calibrated and validated as a function of the catchment shape based on two coefficients: the Gravelius coefficient (K_G – Eq. 4) and the Form coefficient (K_F – Eq. 5). Both coefficients describe the geometry of the catchment area and can be interpreted as how compact the distribution of area is. Commonly linked to flood proneness, these parameters also relate to the transversal distance of the catchment area, which influences the amount of lateral inflow into the mainstream.

$$\lambda = \frac{A_o}{A_m} \tag{3}$$

$$K_G = 0.28 \cdot \frac{C_P}{C_A} \tag{4}$$

$$K_F = \frac{C_A}{C_L^2} \tag{5}$$

In Equation 3, the terms A_o and A_m are the observed and measured cross-section area and in Equations 4 and 5, C_P, C_A and C_L stand for the catchment perimeter, area and length, respectively.

The plots of λ versus both parameters are presented in Figure 5. Two equations ($\lambda(K_G)$ and $\lambda(K_F)$, see Figure 5) were calibrated using data from 14 randomly selected sections out of the 21 assessed by the DEM. The remaining data were used to validate the equations. The model FLM-λ consists of processing the FLM as originally proposed and, afterwards, multiplying the output area by the λ correction parameter. Since $\lambda \geq 1.0$, the multiplication simulates the effect of wall erosion.

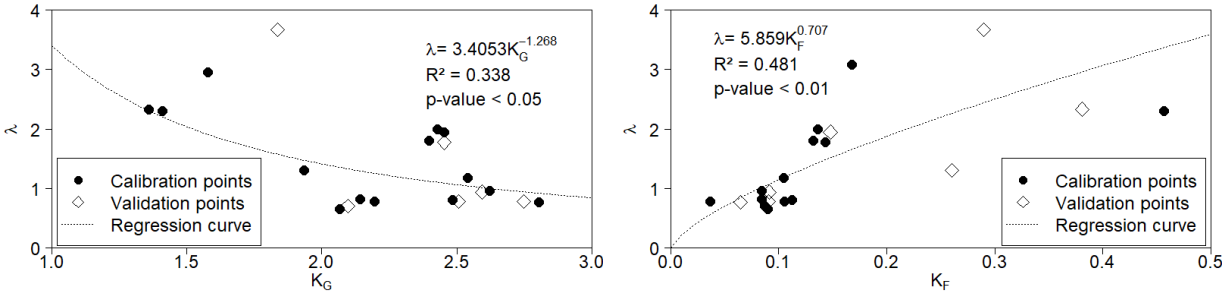

(a) (b)

Figure 5. Correlations between the ratio ($\lambda = A_o/A_m$) and (a) the Gravelius coefficient (K_G) and (b) the form factor (K_F) for 21 monitored cross-sections at MRB. Black dots refer to calibration cross-sections and white diamonds refer to validation cross-sections. The values of R^2 indicated in the plots are for the calibration. The validation R^2 were 0.10 for K_G and 0.54 for K_F.

$$\lambda = \max\left(5.859{K_F}^{0.707}; 1.0\right) \tag{6}$$

The coefficient (K_F) yielded a positive Nash-Sutcliffe Efficiency value and smaller RMSE (0.17 and 0.67, respectively) which did not occur with the Gravelius coefficient (-2.43 and 0.84, respectively). In the revised model, hereafter addressed as FLM-λ, the FLM area output is multiplied by the calibrated parameter λ (Equation 6), yielding the eroded area. Applying this factor caused a significant improvement in model efficiency, with NSE increasing from 0.557 to 0.757. The incremental area produced by the multiplication of λ is assumed to increase the width of the upper half of the cross-section, keeping bottom width and the orthogonality of the walls unchanged.

2.5.2 Coupled Model – Foster and Lane & Sidorchuk Model (FL-SM)

The previous model was produced due to the necessity of considering wall failure as a sediment source and used an empirical approach. Another way, using a physically-based concept, is to include the specific routine of the Sidorchuk model that tackles wall failure in the Foster and Lame model. This can be achieved by simply including a test after each event, checking if the depth of the channel causes wall instability given the current angle of the bank.

By analysing the data, however, we identified that for small cross-sections, even after the critical had been reached, the section remained rectangular. This implies an additional threshold mechanism related to the geometry of the channel and/or catchment. Therefore, the FL-SM requires the determination of a threshold value for the implementation of the wall erosion equations. Such a threshold controls when the wall erosion becomes significant for the total amount of eroded soil. In the model, it represents the limit stage, above which Sidorchuk (1999) equations are used. It also represents the scale when solely the channel bed erosion, described by the Foster and Lane (1983) equations, start to consistently underestimate the measured area. In this study, we used the Foster and Lane model to identify this scale where both processes (channel bed and wall erosion) switch relevance.

A flow chart of the FL-SM is presented below in Figure 6. The core of the model is the Foster and Lane Model, processed for every runoff event. When the cross-section reaches the threshold condition and satisfies the criteria for wall failure as described in Sidorchuk (1999), a new step is included that calculates wall transformation.

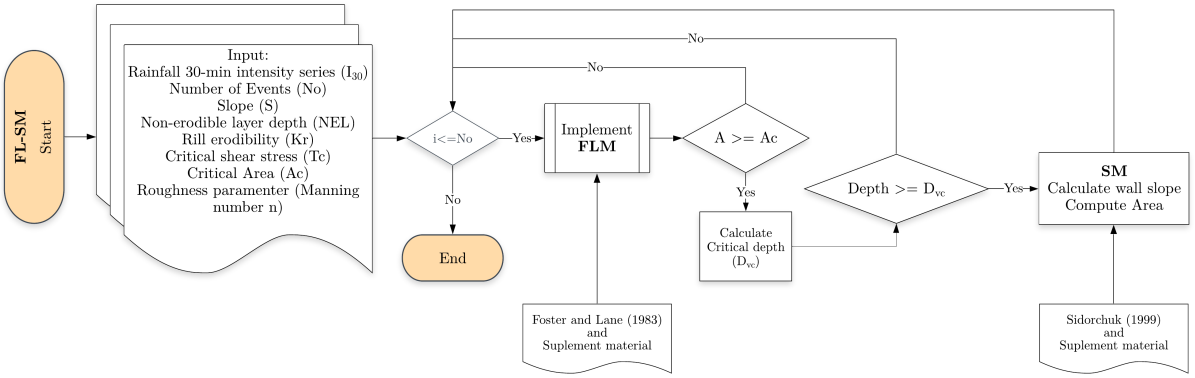

Figure 6. Flow chart of the Coupled model FL-SM.

2.6 Model fitness evaluators

To assess the goodness-of-fit, the Nash-Sutcliffe Efficiency coefficient (NSE), the root mean squared error (RMSE) and the percent bias (PBIAS) were used (see Moriasi et al., 2007). Additionally, the methodology proposed by Ritter and Muñoz-Carpena (2013) asserts statistical significance to the evaluators. The proposed model is based on Monte Carlo sample techniques to reduce subjectivity when assessing the goodness-of-fit of models.

$$NSE = 1 - \frac{\sum_{i=1}^{n}(X_{o,i} - X_{m,i})^2}{\sum_{i=1}^{n}(\bar{X_o} - X_{o,i})^2} \tag{7}$$

$$RMSE = \sqrt{\frac{\sum_{i=1}^{n}(X_{o,i} - X_{m,i})^2}{n}} \tag{8}$$

$$PBIAS = \frac{\sum_{i=1}^{n}(X_{o,i} - X_{m,i})}{\sum_{i=1}^{n}(X_{o,i})} \tag{9}$$

In Equations 7, 8 and 9, $X_{o,i}$ is an observation and $X_{m,i}$ a modelled value, with n being the total of observations and simulations. $\bar{X_o}$ is the average of the observed values.

3 RESULTS

3.1 Gully modelling

From the three gullies measured, twenty-one cross-sections with different dimensions were selected and used to validate and compare the model's quality. Figure 7 presents the scatter of modelled and measured data for the models implemented. The FL-SM presented a Nash-Sutcliffe Efficiency coefficient of 0.846 when using a threshold for the area of the cross-section of 2.2 m^2. In Figure 8, some output examples for the sections above the threshold are presented.

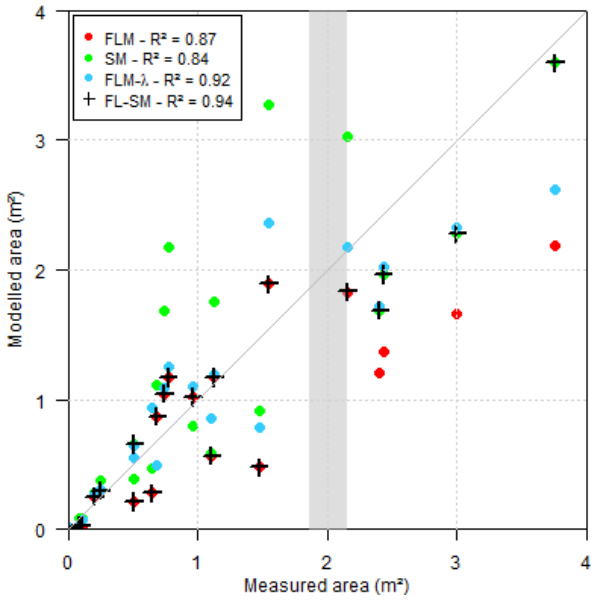

Figure 7. Performance of the coupled model (FL-SM), Foster and Lane Model (FLM and FLM-λ) and the Sidorchuk model (SM). p-value < 0.001 for all sets. The grey bar indicates the identified threshold area where there is a change, and SM becomes consistently better than the FLM.

In terms of geometry, sections models with the Foster and Lane Model with its original formulation present output cross-sections similar to Figure 8 [(a), (b), (c)], with rectangular-live shape. When the parameter λ is introduced (FLM-λ), the output cross-sections are modelled with piled rectangles as in Figure 8 [(d), (e), (f)]. Using the FL-SM, when the area surpasses the threshold value, sections have mainly trapezoidal geometry, as illustrated in Figure 8 [(g), (h), (i)]. It is important to highlight that the model can produce triangular geometry, but none was obtained in this study.

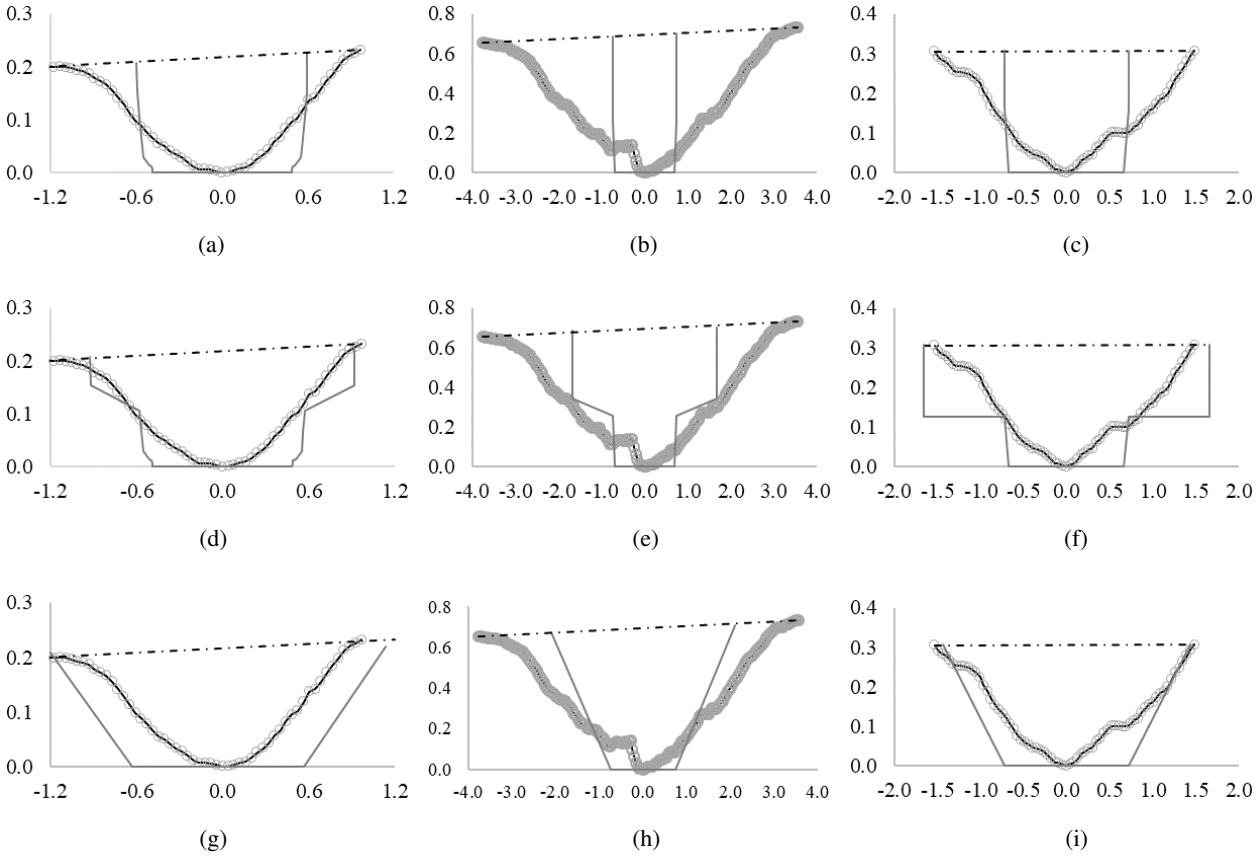

Figure 8. Some examples of gully cross-sections measured (black line with circles) and the modelled (dark grey line) geometry. figures (a), (b) and (c) show the output for the model of Foster and Lane; figures (d), (e) and (f) the output for the model of Foster and Lane adapted with the parameter λ and figures (g), (h) and (i) the result from the Sidorchuk Model (SM). Distances in metres. The section in (a, d and g) is a section obtained from gully 1, (b, e and h) from gully 2, and (c, f and i) from gully 3.

3.1.1 Threshold analysis

The interpretation of the threshold for implementation of the wall erosion routine can be based on (a) the cross-section area or (b) the catchment geometry, as illustrated in Figure 9. The first approach considers a critical area that once reached, marks when the wall erosion is truly significant with respect to the other processes. In this study, the threshold identified was at an area of 2.2 m^2. After that, the model calculates the effect of sidewall erosion and reaches the critical final area for the analysed section. The presence of a threshold for applying the sidewall erosion routine indicates a change of relevance among processes on a given scale. Although the threshold is addressed as an area, this is only a consequence of more complex interactions among discharge, flow erosivity, cohesion and gravitational forces.

The second interpretation is related to the catchment geometry, as the approach given to the parameter λ also related to the K_F. From the distribution of the cross-sections, we can observe sections that are better modelled by SM even below the

threshold. By analysing the values of the form coefficient (K_F) of each set (Figure 9b), we observed that set 1 has K_F of 0.08 ($\pm$ 0.02) and set 2 has 0.22 ($\pm$ 0.12). Higher values of K_F indicate a more compact catchment, with more lateral flux into the channel, therefore producing more erosion in the soil. By sorting the model results of FLM and SM based on the form coefficient, using the threshold of K_F = 0.15, we obtained an NSE of 0.79.

Given the obtained efficiencies, in this study, we adopted a threshold based on the cross-section area. However, the use of a catchment-based threshold should not be discarded and could be promising, since there are reports in literature of the relation between lateral flow and gully erosion (Blong and Veness, 1982).

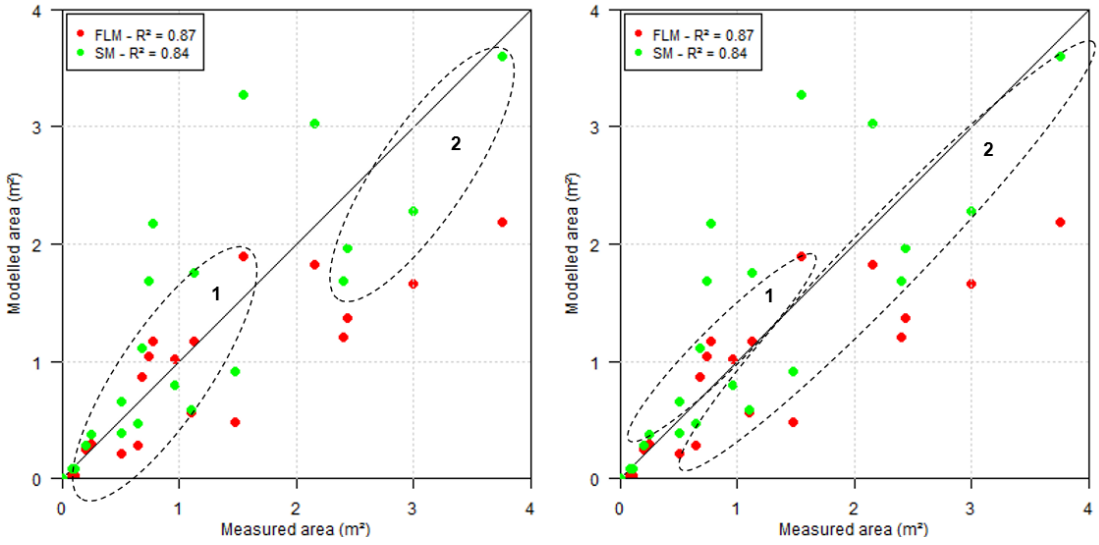

Figure 9. Thresholds for wall erosion: (a) based on the cross-section area; (b) based on the catchment geometry and K_F. In both plots, the set 1 indicates the domain of bed erosion and Foster and Lane equations and set 2 indicates the domain of wall erosion and Sidorchuk equations. p-value < 0.001.

3.1.2 Rainfall intensity

From the three gullies, twenty-one cross-sections with no interference of bushes or trees were selected from the Digital Elevation Model. The FLM was tested for the 60-minute, 30-minute, 15-minute and average intensities [FLM(I_{60}), FLM(I_{30}), FLM(I_{15}), FLM(I_{av})]. The best response was shown when using the thirty-minute intensity [FLM(I_{30}); NSE = 0.557]. Figure 10 presents the plot of the model outputs for the cross-section area compared with the measured data. Moreover, the Foster and Lane Model did not show good responses to the cross-section geometry, regardless of the intensity tested. This may indicate a flaw in the model concerning the side-ward erosive process.

The FLM considers rectangular-shaped cross-sections, but the field survey showed that the sections were rather trapezoidal or triangularly shaped (Figure 8). Among the factors that can shape gully walls, others include seepage, angle of internal

friction, and the slope angle itself (Sidorchuk, 1999; Bingner et al., 2016). Besides this, gully walls can be shaped by lateral discharge (Blong and Veness, 1982) which depends directly on the morphology of the cross-section catchment area. Figure 10 also shows a tendency of the model to underestimate the cross-section area, which implies that the model does not consider all the relevant erosive processes. The sidewall erosion has proven to be a relevant source material, often representing over 50 % of the eroded mass (Crouch, 1987) whereas the FLM only assumes the vertical sidewall morphology. Therefore, in this study, we adopted the 30-minute intensity as the standard intensity and duration to assess peak-discharge.

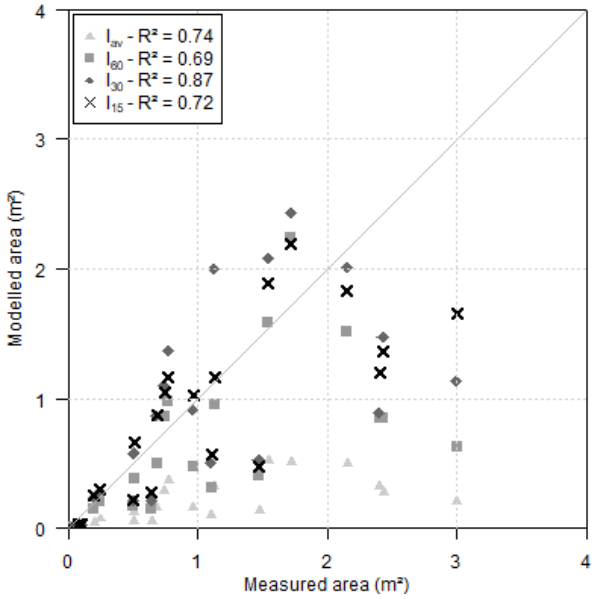

Figure 10. Results of the FLM for cross-section area using different intensities (I_{av} – average; I_{60} – 60-min; I_{30} – 30-min; and I_{15} – 15-min) to generate the peak discharge.

3.2 Model evaluators

The coupled model, FL-SM, presented the highest performance of goodness-of-fit evaluators (Figure 11). The model yielded a PBIAS value below 10 %, which is very good. The coupled-model RMSE was also low (0.397), whereas the NSE reached a value of 0.846, being classified as good (Ritter and Muñoz-Carpena, 2013) or very good (Moriasi et al., 2007).

Figure 11 shows the evolution of NSE values with more details to allow for conclusions be drawn. The Foster and Lane model with λ parameter (FLM-λ) was calibrated with 14 cross-sections out of 21 and performed as well as the Sidorchuk model (SM), which considers the sidewall effect. For the coupled model, there is no efficiency gain when applying the calibrated parameter (λ) to sections below the threshold which indicates that the lateral inflow is only relevant for larger sections. Figure 12 presents the Taylor diagram for comparison of the four models. In this diagram, the closer a model is to the reference (measured data) the better. The FL-SM presented the highest correlation and the lowest RMSE.

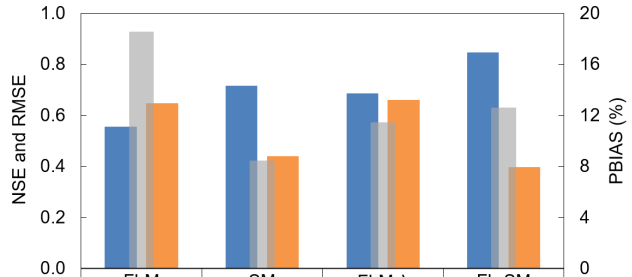

	FLM	SM	FLM-λ	FL-SM
NSE	0.56	0.72	0.69	0.85
RSME	0.65	0.44	0.66	0.40
PBIAS	18.6	8.5	11.5	12.6

Figure 11. Model evaluators NSE, $RMSE$ and $PBIAS$. The bar plot shows the performance of all tested models – values of $PBIAS$ in percentage.

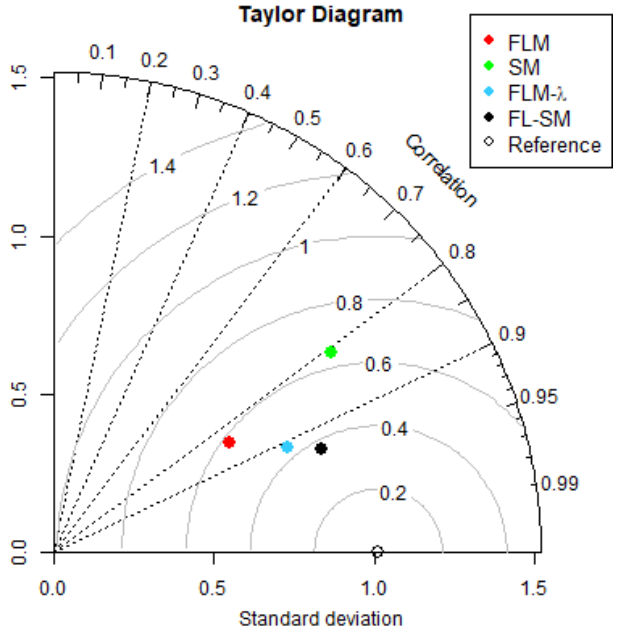

Figure 12. Taylor diagram for the model performance. The azimuthal distance gives the correlation (R - Pearson). The distance to the origin is proportional to the standard deviation of the model values and the distance to the reference (measured data) is proportional to the $RMSE$.

We also used the strategy of Ritter and Muñoz-Carpena (2013), the FITEVAL. The concept behind this strategy is a Monte Carlo approach to the Nash-Sutcliffe Efficiency computation. Using repeated re-sampling from the dataset, their method delivers a probability density function to the NSE. This allows for an uncertainty analysis for the evaluator. The FL-SM presented an NSE $\in$ [0.66;0.95] for a p-value of 0.05, being classified as acceptable to very good. A conservative interpretation of this result implies considering the lowest values as the minimum state of information, or as the one that contain (almost) no unproven

hypothesis. As a consequence, and according to Ritter and Muñoz-Carpena (2013), the FL-SM can be classified as acceptable to very good. The detailed output of the FITEVAL analysis can be found in the supplementary material (Fig. S6).

3.3 Gully growing modelling

Gully growth is commonly described as being a fast process in the first years which progressively slows down its enlargement. In our model, the mechanism that produces this dynamic is event piling. It could be observed that, after a particularly intense event, the channel is sufficiently wide. Therefore, following less intense events produce only shallow flow and low shear stress, producing fewer or no sediment. Only with a more intense event than the last erosive one, there is further erosion.

Our model mimics this growing dynamic and its periods between extreme events. Such behaviour is widely explored in literature (Vanwalleghem et al., 2005; Poesen et al., 2006; Poesen, 2018) and illustrated in Fig. 13. Vanwalleghem et al. (2005), using several data-sets from previous studies, found a strong correlation between GT (the percentage of the gully age over the total) and GV (the percentage of the gully volume over the total), given by a function as expressed in Eq. 10. The parameters α and β were calibrated by Vanwalleghem et al. (2005) as 96.5 and -0.07 with the coefficient of determination (R^2) equal to 0.99.

$$GV = \alpha[1 - \exp(\beta GT)] \tag{10}$$

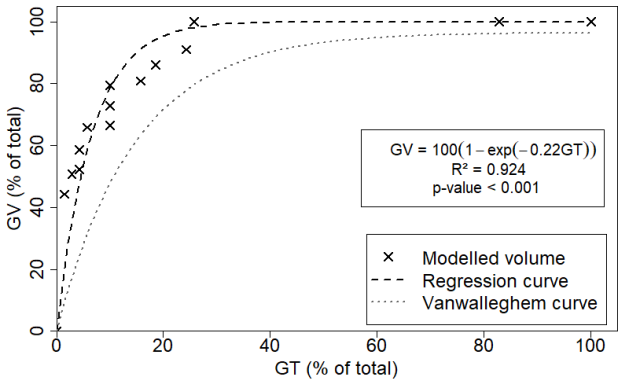

Figure 13. The behaviour of gully growing rate as proposed by literature (Vanwalleghem et al., 2005; Poesen et al., 2006) and modelled (data from Gully 1). GV is the gully volume in percentage and GT the gully age in percentage.

The parameters α (equal to 100) and β (equal to -0.22) obtained in our study differ from the values in literature. While the difference in α is due to a numerical formulation (GV_{total} is equal to the measured volume), the parameter β brings us some insights. Its absolute value for our data set is three times larger than that calibrated by Vanwalleghem et al. (2005). A larger $|\beta|$ indicates a fast initial growth, possibly caused by the intensive rainfall regime of the region, with convective intense events and high erosivity (Medeiros and Araújo, 2014). This is a different condition from Belgium and Russia, where most studies

that lead to Vanwalleghem et al.'s equation were carried out. Therefore, although gully growth behaviour is similar in different regions, local conditions such as climate and land use should be taken into account.

3.4 Landscape development impacts on gully erosion

Gullies are scale-dependent phenomena and frequently related to thresholds due to their initiation, which is based on catchment area and slope (Torri and Poesen, 2014; Poesen, 2018). Both characteristics are directly linked to shear stress and stream power when using physical gully models. Montgomery and Dietrich (1992) argue that changes in the landscape and the drainage system can lead to a larger occurrence of channelisation and its impacts can be noticed faster. Torri and Poesen (2014) suggest a threshold for head development in gullies as conveyed in Equation 11.

$$S\, C_A^{0.38} > k \tag{11}$$

where S (m m^{-1}) is the slope, C_A (ha) is the catchment area and k is a parameter for channel and gully initiation.

For croplands in tropical conditions, the proposed value of k is 0.042 (Torri and Poesen, 2014). For the areas in the present study, we have channel initiation for values lower than half (k = 0.020) and systematically lower than the field data of Vandaele et al. (1996) could be observed. These findings suggest the vulnerability of the region gullying. Considering that the three experimental sites were located next to a road, this disturbance triggered gully initiation and other actions may cause similar problems in the region, such as deforestation and forest fire. The roads have not only enlarged the total catchment area but have also increased its length. While relations between catchment length and area are well-established ($L = b\, c_A^{0.49}$) with values of b varying from 1.78 to 2.02 (Montgomery and Dietrich, 1992; Sassolas-Serrayet et al., 2018), the present experiments found b equalling 3.17. With a smoother surface and almost no meandering, road construction caused modifications that promoted more energetic flows on the gully head. Road construction has also been identified as a potential factor for gully initiation in other areas of the Brazilian Semiarid Region, as in the Salitre Catchment, where large gullies started after construction of an unpaved rural road (da Silva and Rios, 2018).

4 DISCUSSION

4.1 Model limitations

The proposed models, especially the FL-SM, presented a significant improvement, reaching an efficiency over 0.8. Yet, some reflections can be made to understand when the models fail, as well as understand where new advances can be pursued.

4.1.1 Foster and Lane Model (FLM)

The FLM requires a peak discharge duration input. Given the lack of such data in the region, our first step in this study was to identify which was the best peak and duration of rainfall to be considered, based on rainfall intensity. Therefore, a relevant

result from this work is the confirmation that the 30-minute intensity is the one that provides the most information about gully erosion. Wischmeier and Smith (1978) proposed the product of total storm energy and the 30-minute intensity to "predict the long-time average soil loss in runoff". The use of I_{30} for estimating event-related gully erosion was previously experimentally tested by Han et al. (2017). The authors had monitored a gully in the Loess Plateau in China for 12 years, registering 115 erosive rainfall events. They concluded that the product of 30-minute intensity and total precipitation ($P\,I_{30}$) was the key parameter to estimate total soil loss. Our results corroborate this.

Furthermore, by applying the I_{30} in this study in order to estimate peak discharge and duration, it is implied that all the energy necessary to initiate and develop a gully channel comes from the most intense 30 minutes. Due to the limited number of gullies, it is not straightforward that the I_{30} could be the most representative index for any situation. Peak discharge and critical rainfall duration are often central variables in gully models (Foster and Lane, 1983; Hairsine and Rose, 1992; Sidorchuk, 1999; Gordon et al., 2007) and are related to erosion initiation parameters and thresholds, such as shear stress and stream power. This second factor has frequently been reported in literature as being more correlated with both laminar and linear erosion (Bennett and Wells, 2019). Figure 10a shows the performance of the tested intensities. Although the model using the 15-minute intensity presented smaller PBIAS and RMSE, the results indicated a large scatter around average.

Finally, the Foster and Lane Model also considers a fixed shear distribution, which is often unrealistic (Bonakdari et al., 2014) and has a fixed rectangular shape that, although frequently accurate for ephemeral gullies, does not agree with field data and literature (Fig. 8; Starkel, 2011).

4.1.2 Sidorchuk Model (SM)

The SM produced good results in this study which were similar to those obtained by inserting a calibrated factor (λ) in FLM. It is important to note that the original model used empirical correlations to determine width (Sidorchuk, 1999; Nachtergaele et al., 2002) and these were obtained using data from the Yamal basin. In the present study, we substituted this approximation for the width estimated by the FLM model, which permitted a more physical approach and increased the quality of the SM. The model was also capable to predict the sidewall slope well.

The model, however, showed a trend of overestimating smaller cross-sections (see Figure 7) mainly due to section geometry. When applied, the bottom width of the channel is considered to be the final width obtained by FLM. In larger sections, this hypothesis holds once the discharge is large enough to carry all soil produced by sidewall erosion. In smaller sections, part of the soil is deposited and produces a V or U-shaped cross-section (Starkel, 2011).

4.1.3 Proposed Models

The FLM was further improved by the addition of the calibrated parameter λ (FLM-λ). This parameter was included to predict the effect of lateral discharges over wall erosion. Due to the significant improvement produced by its insertion, it could be understood that the original FLM fails to tackle this source of material (Blong and Veness, 1982; Crouch, 1987).

The FL-SM considers two sediment sources: channel bed and sidewall. Gullies are, however, complex systems with many sources and interactions. Headcut, sidewall erosion due to raindrops, flow jets and piping were not considered in our modelling

approach. Processes of infiltration, subsurface flow and transport capacity were also neglected and should be properly addressed in future works. Nevertheless, the FL-SM assumptions managed to mimic the field measurements well, which implies that, at least in this study, the neglected processes are of lower relevance or were considered indirectly. For instance, sidewall erosion by raindrops can be considered insignificant over the wall failure process considered by Sidorchuk (1999). In addition, it is important to notice that, by selecting the 30-minute intensity, a less intense interval might be overlooked that also produces erosive discharge, and can, therefore, explain the remaining processes.

One advantage of the FLM-λ over the FL-SM is that the former requires less data than the latter. The Sidorchuk model, and consequently the FL-SM require extra fieldwork and laboratory analysis to assess root mass and plasticity index.

Despite the good results obtained from the modelling, the use of stochastic approaches and introduction of other sources of sediment(Sidorchuk, 2005) should improve the performance of the model. This is also relevant for generalisation and modelling of classical gullies. In the same way, the introduction of processes such as armouring and energy losses, as proposed by Hairsine and Rose (1992), can be interpreted as probabilistic terms.

Comparatively, with other models, either physical or empirical (Hairsine and Rose, 1992; Woodward, 1999; Wells et al., 2013; Dabney et al., 2015), our proposed model (FL-SM) requires a similar or less amount of data, little calibration (one parameter – the threshold) and is more versatile. Most models fail to account for multiple rainfall events (Foster and Lane, 1983; Woodward, 1999; Nachtergaele et al., 2002) and to consider multiple sources of sediment (Foster and Lane, 1983; Hairsine and Rose, 1992; Dabney et al., 2015). The FL-SM model (R^2 = 0.94) presented a better performance index than empirical models [e.g. R^2: 0.55 and 0.12 for Woodward (1999) and Wells et al. (2013) respectively] and physical models [e.g. R^2: 0.87 and 0.84 for Foster and Lane (1983) and Sidorchuk (1999) respectively]. This enhancing in the performance can be accounted for by the more detailed modelling, considering wall failure and non-rectangular cross-section.

4.2 Data limitations

4.2.1 Topographic data

In terms of accuracy and agility, a topographic survey with UAV permits to measure sites within a few minutes. Conventional measurements, such as those with total station or profilometer, are more time consuming and do not grant better resolutions. The UAV accuracy, however, can be enhanced by performing flights in lower heights and with more GCPs (Agüera-Vega et al., 2017; James et al., 2017), as well as by using high-end equipment, such as more robust UAVs and stabilizers. Total stations can also be used to improve the accuracy of ground control points (Mesas-Carrascosa et al., 2016). Given the scale of this study and the presented results of the models, the four-centimetre pixel represents a good resolution, since it combines good precision with affordable computational costs (Wang et al., 2016). The solution of UAV-based volume assessment is a good option for monitoring gully evolution (Stöcker et al., 2015), allowing frequent surveys, e.g., after every intense rainfall event.

However, trees and bushes obscure topographic measurements if too close to the gully channel and/or too dense in the catchment. Thus, UAV monitoring is more reliable for gully sites in non- or meagre-vegetated areas and meadows, which combines with the conditions of this study, except for gully 3 (G3), where it was impossible to accurately measure the total

erosion volume due to relatively dense vegetation. It was, however, possible to select a large enough number of sections (eight) at G3 to assess the total erosion volume.

The topographic survey showed that all gullies had a significant portion of their watersheds occupied by the road, indicating a modification of the drainage system and change in the catchment boundaries – both causes of gully initiation foreseen by Ireland et al. (1939) – due to road construction, which promoted intense runoff and triggered gullies. Impacts of road construction on gully formation were also observed in Ethiopia (Nyssen et al., 2002) and the USA (Katz et al., 2014). Considering such previous records in literature and the information collected from locals, the modelling considered 1958 as the start of gully erosion, coinciding with road construction.

4.3 Soil data

Though the three studied gullies are located in the same mesoscale basin, the Caatinga biome is known for its soil variability (Güntner and Bronstert, 2004) and soil properties do differ among the gullies. However, only small changes of texture were observed in different depths, allowing an analysis based on average properties. Nevertheless, for deeper and/or more variable soils, the discretization of soil properties, and therefore parameters such as rill erodibility (K_r) and critical shear stress (τ_c), can easily be taken into account. The good performance of the final model (FL-SM) also indicates that the WEPP equations for critical shear stress and rill erodibility (Eq. 1 and 2) can be used for the soils of the region. These equations were obtained via regression curves from data collected on 34 plot areas in the USA with a wide range of textures, slopes, land use and land cover. The areas from the WEPP model possess different geological and climatic conditions from the soils in the Brazilian semiarid region; this is why local studies should be carried out, given that empirical equations frequently have strong local character (Ghorbani-Dashtaki et al., 2016; Dionizio and Costa, 2019).

4.4 Rainfall data

This study shows that sub-daily information of rainfall is of crucial importance for gully modelling. In this study, we used correlation curves based on long-term time series of a similar catchment in the region. However, such analysis might introduce an averaged and monotonic behaviour for the intensities, as presented in Figure 4, and is, therefore, unrealistic. Stochastic models should be tested to estimate sub-daily information from daily rainfall. The estimation of discharge from rainfall can also be improved by considering water content in the soil and modelling its evolution over the studied period using water balance models.

5 Conclusions

In this study, we proposed and tested two new gully models based on two previous models (Foster and Lane, 1983 and Sidorchuk, 1999). We also investigated which rainfall intensity is best suit for gully modelling when sub-daily rainfall data is not available, finding the 30-minute intensity (I_{30}) to be the most appropriate.

The models present a significant improvement when compared to other models in literature. While the FLM-λ requires less calibration, the FL-SM presented better results, not only in terms of total gross erosion, but also in terms of gully growing dynamic. Through modelling and fieldwork, it was also possible to identify the effects of landscape change and climatic conditions on gully development in the region. Gully is an erosion related to many processes and it is scale-dependent. The attempt of proposing a generalist model for gullies should also consider these different scales and mechanisms involved in different stages of the gully development. Catchment shape and lateral flow have a central role in gully erosion and their influence should be further investigated. Infrastructure construction, like roads, changes conditions for gully initiation and was the trigger for the studied gullies.

Nonetheless, further efforts are required to fully model gully erosion, such as include the multiple other sources including headcut, pipping, channel shear stress and flow jets. Also, stochastic modelling should be implemented in order to tackle inherent uncertainties of many sediment sources and lack of data.

Code and data availability. Code and data available in the link: https://github.com/PedroAlencarTUB/GullyModel-FLSM

Author contributions. Alencar worked on fieldwork, programming and laboratory analysis. Teixeira carried out image acquisition and processing. de Araújo acted as supervisor of the work and in its conceptualisation. Alencar prepared the text with contributions of all authors.

Competing interests. The authors declare that they have no conflict of interest.

This work is part of the PhD work of **Pedro Alencar** and will be used in his dissertation.

Disclaimer.

Acknowledgements. This study was partly financed by the *Coordenação de Aperfeiçoamento de Pessoal de Nível Superior - Brasil* (CAPES) - Finance Code 001, Capes/Print Grant 88881.311770/2018-01 and by the *Edital Universal* CNPq - number 407999/2016-7. Pedro Alencar is funded by the DAAD – Award Number: 91693642. Many thanks to Prof. Eva Paton for the support and advising at the Technische Universität Berlin.

References

Agüera-Vega, F., Carvajal-Ramírez, F., and Martínez-Carricondo, P.: Assessment of photogrammetric mapping accuracy based on variation ground control points number using unmanned aerial vehicle, Measurement, 98, 221–227, 2017.

Alberts, E. E., Nearing, M. A., Weltz, M. A., Risse, L. M., Pierson, F. B., Zhang, X. C., Laflen, J. M., and Simanton, J. R.: Soil Component, Tech. Rep. July, USDA, 1995.

Arabameri, A., Cerda, A., and Tiefenbacher, J. P.: Spatial Pattern Analysis and Prediction of Gully Erosion Using Novel Hybrid Model of Entropy-Weight of Evidence, Water, 11, 1129, 2019.

Azareh, A., Rahmati, O., Rafiei-Sardooi, E., Sankey, J. B., Lee, S., Shahabi, H., and Ahmad, B. B.: Modelling gully-erosion susceptibility in a semi-arid region, Iran: Investigation of applicability of certainty factor and maximum entropy models, Science of the Total Environment, https://doi.org/10.1016/j.scitotenv.2018.11.235, 2019.

Bennett, S. J. and Wells, R. R.: Gully erosion processes, disciplinary fragmentation, and technological innovation, Earth Surface Processes and LandformsBeschuldigung, 44, 46–53, https://doi.org/10.1002/esp.4522, 2019.

Bernard, J., Lemunyon, J., Merkel, B., Theurer, F., Widman, N., Bingner, R., Dabney, S., Langendoen, E., Wells, R., and Wilson, G.: Ephemeral Gully Erosion — A National Resource Concern., U.S. Department of Agriculture. NSL Technical Research Report No. 69, p. 67 pp, 2010.

Bingner, R. L., Wells, R. R., Momm, H. G., Rigby, J. R., and Theurer, F. D.: Ephemeral gully channel width and erosion simulation technology, Natural Hazards, 80, 1949–1966, https://doi.org/10.1007/s11069-015-2053-7, 2016.

Blong, R. J. and Veness, J. A.: The Role of Sidewall Processes in Gully Development, Earth Surface Processes and Landforms, 7, 381–385, 1982.

Bonakdari, H., Sheikh, Z., and Tooshmalani, M.: Comparison between Shannon and Tsallis entropies for prediction of shear stress distribution in open channels, Stochastic Environmental Research and Risk Assessment, 29, 1–11, https://doi.org/10.1007/s00477-014-0959-3, 2014.

Borrelli, P., Robinson, D. A., Fleischer, L. R., Lugato, E., Ballabio, C., Alewell, C., Meusburger, K., Modugno, S., Schütt, B., Ferro, V., Bagarello, V., Oost, K. V., Montanarella, L., and Panagos, P.: An assessment of the global impact of 21st century land use change on soil erosion, Nature Communications, 8, https://doi.org/10.1038/s41467-017-02142-7, 2017.

Castillo, C. and Gómez, J. A.: A century of gully erosion research: Urgency, complexity and study approaches, Earth-Science Reviews, 160, 300–319, https://doi.org/10.1016/j.earscirev.2016.07.009, 2016.

Chow, V. T.: Open-channel hydraulics, in: Open-channel hydraulics, McGraw-Hill, 1959.

Coelho, C., Heim, B., Foerster, S., Brosinsky, A., and de Araújo, J. C.: In situ and satellite observation of CDOM and chlorophyll-a dynamics in small water surface reservoirs in the brazilian semiarid region, Water (Switzerland), 9, https://doi.org/10.3390/w9120913, 2017.

Conoscenti, C. and Rotigliano, E.: Predicting gully occurrence at watershed scale: Comparing topographic indices and multivariate statistical models, Geomorphology, 359, 107 123, https://doi.org/10.1016/j.geomorph.2020.107123, 2020.

Crouch, R. J.: The relationship of gully sidewall shape to sediment production, Australian Journal of Soil Research, 25, 531–539, 1987.

da Silva, A. J. P. and Rios, M. L.: Alerta de desertificação no médio curso do Rio Salitre, afluente do Rio São Francisco, Tech. rep., IFBA, Senhor do Bonfim, Bahia, 2018.

Dabney, S. M., Vieira, D. A. N., Yoder, D. C., Langendoen, E. J., Wells, R. R., and Ursic, M. E.: Spatially Distributed Sheet, Rill, and Ephemeral Gully Erosion, Journal of Hydrologic Engineering, 20, C4014 009, 2015.

de Araújo, J. C. and Piedra, J. I. G.: Comparative hydrology: analysis of a semiarid and a humid tropical watershed, Hydrological Process, 23, 1169–1178, https://doi.org/10.1002/hyp, 2009.

de Araújo, J. C., Güntner, A., and Bronstert, A.: Loss of reservoir volume by sediment deposition and its impact on water availability in semiarid Brazil / Perte de volume de stockage en réservoirs par sédimentation et impact sur la disponibilité en eau au Brésil semi-aride Loss of reservoir volume by se, Hydrological Sciences Journal, 51, 157–170, https://doi.org/10.1623/hysj.51.1.157, 2006.

Dionizio, E. A. and Costa, M. H.: Influence of Land Use and Land Cover on Hydraulic and Physical Soil Properties at the Cerrado Agricultural Frontier, Agriculture, 9, 14, https://doi.org/10.3390/agriculture9010024, 2019.

dos Santos, J. C. N., de Andrade, E. M., Guerreiro, M. J. S., Medeiros, P. H. A., de Queiroz Palácio, H. A., and de Araújo Neto, J. R.: Effect of dry spells and soil cracking on runoff generation in a semiarid micro watershed under land use change, Journal of Hydrology, 541, 1–10, https://doi.org/10.1016/j.jhydrol.2016.08.016, 2016.

Figueiredo, J. V., Araújo, J. C., Medeiros, P. H. A., and Costa, A. C.: Runoff initiation in a preserved semiarid Caatinga small watershed, Northeastern Brazil, Hydrological Processes, 30, 2390–2400, https://doi.org/10.1002/hyp.10801, 2016.

Foster, G. R. and Lane, L. J.: Erosion by concentrated flow in farm fields, in: D.B. Simons Symposium on Erosion and Sedimentation, p. 21, 1983.

Gaiser, T., Krol, M., Frischkom, H., and de Araujo, J. C., eds.: Global Change and Regional Impacts, Springer-Verlag, Berlin, https://doi.org/10.1007/978-3-642-55659-3_9, 2003.

Ghorbani-Dashtaki, S., Homaee, M., and Loiskandl, W.: Towards using pedotransfer functions for estimating infiltration parameters, Hydrological Sciences Journal, 61, 1477–1488, https://doi.org/10.1080/02626667.2015.1031763, 2016.

Gordon, L. M., Bennett, S. J., Bingner, R. L., Theurer, F. D., and Alonso, C. V.: Simulating Ephemeral Gully Erosion in AnnAGNPS, Transactions of the ASAE, 50, 857–866, 2007.

Güntner, A. and Bronstert, A.: Representation of landscape variability and lateral redistribution processes for large-scale hydrological modelling in semi-arid areas, Journal of Hydrology, 297, 136–161, https://doi.org/10.1016/j.jhydrol.2004.04.008, 2004.

Hairsine, P. B. and Rose, C. W.: Modeling water erosion due to overland flow using physical principles: 2. Rill flow, Water Resources Research, 28, 245–250, https://doi.org/10.1029/91WR02381, 1992.

Han, Y., li Zheng, F., and meng Xu, X.: Effects of rainfall regime and its character indices on soil loss at loessial hillslope with ephemeral gully, Journal of Mountain Science, 14, 527–538, https://doi.org/10.1007/s11629-016-3934-2, 2017.

Hunke, P., Mueller, E. N., Schröder, B., and Zeilhofer, P.: The Brazilian Cerrado: Assessment of water and soil degradation in catchments under intensive agricultural use, Ecohydrology, 8, 1154–1180, https://doi.org/10.1002/eco.1573, 2015.

Ireland, H., Sharpe, C. F. S., and Eargle, D. H.: Principles of Gully Erosion in the Piedmont of South Carolina, Tech. rep., USDA, Washington, 1939.

James, M. R., Robson, S., Oleire-Oltmanns, S., and Niethammer, U.: Geomorphology Optimising UAV topographic surveys processed with structure-from-motion : Ground control quality , quantity and bundle adjustment, Geomorphology, 280, 51–66, 2017.

Katz, H. A., Daniels, J. M., and Ryan, S.: Slope-area thresholds of road-induced gully erosion and consequent hillslope-channel interactions, Earth Surface Processes and Landforms, 39, 285–295, https://doi.org/10.1002/esp.3443, 2014.

Liu, X. L., Tang, C., Ni, H. Y., and Zhao, Y.: Geomorphologic analysis and a physico-dynamic characteristics of Zhatai-Gully debris flows in SW China, Journal of Mountain Science, 13, 137–145, 2016.

Maetens, W., Vanmaercke, M., Poesen, J., Jankauskas, B., Jankauskiene, G., and Ionita, I.: Effects of land use on annual runoff and soil loss in Europe and the Mediterranean: A meta-analysis of plot data, Progress in Physical Geography, 36, 599–653, https://doi.org/10.1177/0309133312451303, 2012.

Medeiros, P. H. A. and Araújo, J. C. D.: Temporal variability of rainfall in a semiarid environment in Brazil and its effect on sediment transport processes, Journal of Soils and Sediments, pp. 1216–1223, https://doi.org/10.1007/s11368-013-0809-9, 2014.

Mendes, F. J.: Uma Proposta de Reclassificação das Regiões Pluviometricamente Homogêneas do Estado do Ceará, Dissertação, Universidade Estadual do Ceará, 2010.

Mesas-Carrascosa, F. J., García, M. D. N., De Larriva, J. E. M., and García-Ferrer, A.: An analysis of the influence of flight parameters in the generation of unmanned aerial vehicle (UAV) orthomosaicks to survey archaeological areas, Sensors (Switzerland), 16, 2016.

Montgomery, D. and Dietrich, W.: Channel Initiation and Problem of Landscape Scale, Science, 255, 826–830, 1992.

Montgomery, D. R.: Dirt: The Erosion of Civilizations, universit y of california press, Berkeley, 2007.

Moriasi, D. N., Arnold, J. G., Van Liew, M. W., Bingner, R. L., Harmel, R. D., and Veith, T. L.: Model Evaluation Guidelines for Systematic Quantification of Accuracy in Watershed Simulations, Transactions of the ASABE, 50, 885–900, 2007.

Mutti, P. R., Lúcio, P. S., Dubreuil, V., and Bezerra, B. G.: NDVI time series stochastic models for the forecast of vegetation dynamics over desertification hotspots, International Journal of Remote Sensing, 41, 2759–2788, https://doi.org/10.1080/01431161.2019.1697008, 2020.

Nachtergaele, J., Poesen, J., Sidorchuk, A., and Torri, D.: Prediction of concentrated flow width in ephemeral gully channels, Hydrological Processes, 16, 1935–1953, https://doi.org/10.1002/hyp.392, 2002.

Nkonya, E., Anderson, W., Kato, E., Koo, J., Mirzabaev, A., von Braun, J., and Meyer, S.: Global Cost of Land Degradation, in: Economics of Land Degradation and Improvement - A Global Assessment for Sustainable Development, edited by Nkonya, E., Mirzabaev, A., and von Braun, J., chap. 6, pp. 117–165, Springer Open, Cham, https://doi.org/10.1007/978-3-319-19168-3, 2016.

Nyssen, J., Poesen, J., Moeyersons, J., Luyten, E., Veyret-Picot, M., Deckers, J., Haile, M., and Govers, G.: Impact of Road Building on Gully Erosion Risk: a Case of Study from the Northern Ethiopian Highlands, Earth Surface Processes and Landforms, 27, 1267–1283, 2002.

Panagos, P., Ballabio, C., Meusburger, K., Spinoni, J., Alewell, C., and Borrelli, P.: Towards estimates of future rainfall erosivity in Europe based on REDES and WorldClim datasets, Journal of Hydrology, 548, 251–262, https://doi.org/10.1016/j.jhydrol.2017.03.006, 2017.

Paton, E. N., Smetanová, A., Krueger, T., and Parsons, A.: Perspectives and ambitions of interdisciplinary connectivity researchers, Hydrology and Earth System Sciences, 23, 537–548, https://doi.org/10.5194/hess-23-537-2019, 2019.

Pinheiro, E. A. R., Costa, C. A. G., and Araújo, J. C. D.: Effective root depth of the Caatinga biome, Arid Environments, 89, 4, 2013.

Pinheiro, E. A. R., Metselaar, K., de Jong van Lier, Q., and de Araújo, J. C.: Importance of soil-water to the Caatinga biome, Brazil, Ecohydrology, 9, 1313–1327, https://doi.org/10.1002/eco.1728, 2016.

Poesen, J.: Soil erosion in the Anthropocene: Research needs, Earth Surface Processes and Landforms, 43, 64–84, https://doi.org/10.1002/esp.4250, 2018.

Poesen, J., Vanwalleghem, T., De Vente, J., Knapen, A., Verstraeten, G., and Martínez-Casasnovas, J. A.: Gully Erosion in Europe, in: Soil Erosion in Europe, chap. 39, pp. 515–536, John Wiley & Sons Ltd, https://doi.org/10.1002/0470859202.ch39, 2006.

Ritter, A. and Muñoz-Carpena, R.: Performance evaluation of hydrological models : Statistical significance for reducing subjectivity in goodness-of-fit assessments, Journal of Hydrology, 480, 33–45, https://doi.org/10.1016/j.jhydrol.2012.12.004, 2013.

Sartori, M., Philippidis, G., Ferrari, E., Borrelli, P., Lugato, E., Montanarella, L., and Panagos, P.: A linkage between the biophysical and the economic: Assessing the global market impacts of soil erosion, Land Use Policy, 86, 299–312, 2019.

Sassolas-Serrayet, T., Cattin, R., and Ferry, M.: The shape of watersheds, Nature Communications, 9, 1–8, 2018.

Sena, A., Barcellos, C., Freitas, C., and Corvalan, C.: Managing the health impacts of drought in Brazil, International Journal of Environmental Research and Public Health, 11, 10 737–10 751, https://doi.org/10.3390/ijerph111010737, 2014.

Sidorchuk, A.: Dynamic and static models of gully erosion, Catena, 37, 401–414, https://doi.org/10.1016/S0341-8162(99)00029-6, 1999.

Sidorchuk, A.: Stochastic components in the gully erosion modelling, Catena, 63, 299–317, 2005.

Silva, E., Gorayeb, A., and de Araújo, J.: Atlas socioambiental do Assentamento 25 de Maio-Madalena-Ceará, Fortaleza: Ed. Expressão Gráfica, 2015.

Starkel, L.: Paradoxes in the development of gullies, Landform Analysis, 17, 11–13, 2011.

Stöcker, C., Eltner, A., and Karrasch, P.: Measuring gullies by synergetic application of UAV and close range photogrammetry - A case study from Andalusia, Spain, Catena, 132, 1–11, https://doi.org/10.1016/j.catena.2015.04.004, 2015.

Thompson, J. R.: Quantitative Effect of Watershed Variables on Rate of Gully-Head Advancement, Transactions of the ASAE, 7, 0054–0055, 1964.

Torri, D. and Poesen, J.: A review of topographic threshold conditions for gully head development in different environments, Earth Science Reviews, 130, 73–85, https://doi.org/10.1016/j.earscirev.2013.12.006, 2014.

Valentin, C., Poesen, J., and Li, Y.: Gully erosion: Impacts, factors and control, Catena, 63, 132–153, 2005.

van Schaik, N. L., Bronstert, A., de Jong, S. M., Jetten, V. G., van Dam, J. C., Ritsema, C. J., and Schnabel, S.: Process-based modelling of a headwater catchment in a semi-arid area: The influence of macropore flow, Hydrological Processes, 28, 5805–5816, 2014.

Vandaele, K., Poesen, J. A. W., Govers, G., and van Wesemael, B.: Geomorphic threshold conditions for ephemeral gully incision, Geomorphology, 16, 161–173, 1996.

Vanmaercke, M., Poesen, J., Van Mele, B., Demuzere, M., Bruynseels, A., Golosov, V., Bezerra, J. F. R., Bolysov, S., Dvinskih, A., Frankl, A., Fuseina, Y., Guerra, A. J. T., Haregeweyn, N., Ionita, I., Makanzu Imwangana, F., Moeyersons, J., Moshe, I., Nazari Samani, A., Niacsu, L., Nyssen, J., Otsuki, Y., Radoane, M., Rysin, I., Ryzhov, Y. V., and Yermolaev, O.: How fast do gully headcuts retreat?, Earth-Science Reviews, 154, 336–355, https://doi.org/10.1016/j.earscirev.2016.01.009, 2016.

Vannoppen, W., De Baets, S., Keeble, J., Dong, Y., and Poesen, J.: How do root and soil characteristics affect the erosion-reducing potential of plant species?, Ecological Engineering, 109, 186–195, https://doi.org/10.1016/j.ecoleng.2017.08.001, 2017.

Vanwalleghem, T., Poesen, J., Nachtergaele, J., Deckers, J., and Eeckhaut, M. V. D.: Reconstructing rainfall and land-use conditions leading to the development of old gullies, The Holocene, 15, 378–386, 2005.

Verstraeten, G., Bazzoffi, P., Lajczak, A., Rãdoane, M., Rey, F., Poesen, J., and De Vente, J.: Reservoir and Pond Sedimentation in Europe, Soil Erosion in Europe, pp. 757–774, https://doi.org/10.1002/0470859202.ch54, 2006.

Wang, R., Zhang, S., Pu, L., Yang, J., Yang, C., Chen, J., Guan, C., Wang, Q., Chen, D., Fu, B., and Sang, X.: Gully Erosion Mapping and Monitoring at Multiple Scales Based on Multi-Source Remote Sensing Data of the Sancha River Catchment, Northeast China, ISPRS International Journal of Geo-Information, 5, 200, https://doi.org/10.3390/ijgi5110200, 2016.

Wei, R., Zeng, Q., Davies, T., Yuan, G., Wang, K., Xue, X., and Yin, Q.: Geohazard cascade and mechanism of large debris flows in Tianmo gully, SE Tibetan Plateau and implications to hazard monitoring, Engineering Geology, 233, 172–182, 2018.

Wells, R. R., Momm, H. G., Rigby, J. R., Bennett, S. J., Bingner, R. L., and Dabney, S. M.: An empirical investigation of gully widening rates in upland concentrated flows, Catena, 101, 114–121, https://doi.org/10.1016/j.catena.2012.10.004, 2013.

Wischmeier, W. H. and Smith, D. D.: Predicting rainfall erosion losses - a guide to conservation planning, Tech. rep., USDA, Hyattsville, 1978.

Woodward, D. E.: Method to predict cropland ephemeral gully erosion, Catena, 37, 393–399, 1999.

Yibeltal, M., Tsunekawa, A., Haregeweyn, N., Adgo, E., Meshesha, D. T., Aklog, D., Masunaga, T., Tsubo, M., Billi, P., Vanmaercke, M., Ebabu, K., Dessie, M., Sultan, D., and Liyew, M.: Analysis of long-term gully dynamics in different agro-ecology settings, Catena, 179, 160–174, https://doi.org/10.1016/j.catena.2019.04.013, 2019.

Zhang, S., Foerster, S., Medeiros, P., de Araújo, J. C., and Waske, B.: Effective water surface mapping in macrophyte-covered reservoirs in NE Brazil based on TerraSAR-X time series, International Journal of Applied Earth Observation and Geoinformation, 69, 41–55, https://doi.org/10.1016/j.jag.2018.02.014, 2018.

Zweig, R., Filin, S., Avni, Y., Sagy, A., and Mushkin, A.: Land degradation and gully development in arid environments deduced by mezzo- and micro-scale 3-D quantification – The Negev Highlands as a case study, Journal of Arid Environments, 153, 52–65, https://doi.org/10.1016/j.jaridenv.2017.12.006, 2018.